Acta Crystallographica Section D
Biological Crystallography
ISSN 0907-4449

Structure of Fab hGR-2 F6, a competitive antagonist of the glucagon receptor

Lisa M. Wright,[a] A. Marek Brzozowski,[a] Roderick E. Hubbard,[a] Ashley C. W. Pike,[a] Shirley M. Roberts,[a] Randi Nicoline Skovgaard,[b] Ivan Svendsen,[b] Henrik Vissing[b] and Robert P. Bywater[c]*

[a]York Structural Biology Laboratory, Department of Chemistry, University of York, York YO10 5DD, England, [b]Pharmaceutical Biotechnology, Novo Nordisk A/S, Novo Allé, DK-2880 Bagsværd, Denmark, and [c]Biostructure Department, Novo Nordisk A/S, Novo Nordisk Park, DK-2760 Måløv, Denmark.

Correspondence e-mail: byw@novo.dk

Received 14 July 1999
Accepted 9 March 2000

PDB Reference: Fab hGR-2 F6, 1dqd.

The monoclonal antibody hGR-2 F6 has been raised against the human glucagon receptor and shown to act as a competitive antagonist. As a first step in the structural characterization of the receptor, the crystal structure of the Fab fragment from this antibody is reported at 2.1 Å resolution. The hGR-2 F6 Fab crystallizes in the orthorhombic space group $P2_12_12$, with unit-cell parameters a = 76.14, b = 133.74, c = 37.46 Å. A model generated by homology modelling was used as an aid in the chain-tracing and the Fab fragment structure was subsequently refined (final R factor = 21.7%). The structure obtained exhibits the typical immunoglobulin fold. Complementarity-determining regions (CDRs) L1, L2, L3, H1 and H2 could be superposed onto standard canonical CDR loops. The H3 loop could be classified according to recently published rules regarding loop length, sequence and conformation. This loop is 14 residues long, with an approximate β-hairpin geometry, which is distorted somewhat by the presence of two *trans* proline residues at the beginning of the loop. It is expected that this H3 loop will facilitate the design of synthetic probes for the glucagon receptor that may be used to investigate receptor activity.

1. Introduction

While the rate at which determination of crystal structures of water-soluble globular proteins grows apace, progress in the determination of membrane-protein structures has been very slow. This is a consequence of several factors. Firstly, most membrane proteins, such as G-protein coupled receptors (GPCRs), ion channels and membrane-anchored hormone receptors, act in some kind of signalling capacity and as such are required by the cell in only relatively small amounts compared with many other types of protein. The membrane location also imposes restrictions as to how many protein molecules can be physically accommodated; this will typically be less than 10% of the cell volume.[1] This is in contrast to many water-soluble globular proteins, especially those secreted by the cell, where there are no restrictions to the space available to accommodate the protein within the cell and hence overexpression can more easily be accomplished. Secondly, integral membrane proteins are optimized for compatibility with the membrane environment. Attempts at purifying integral membrane proteins necessarily involve

[1] For a hypothetical spherical cell of radius 1 µm and membrane thickness 3 nm, the membrane occupies 8.7% of the total cell volume. There is of course additional lipid bilayer material inside the cell, but the membrane receptors, which are of interest in structural biology, will be confined within this volume in various pools of receptor within the cell.

disruption of this environment (*e.g.* through the use of detergents and aqueous solvent conditions). Difficulties are also encountered in reconstituting the expressed protein in quantities sufficient for crystallization.

A technique has been developed which can overcome these problems. In this technique, an antibody is raised against the receptor of interest and this antibody can then be used as an immunosorbent for affinity purification of the receptor. Following this, the receptor can be characterized immunologically and structurally. Examples of cases where polyclonal and monoclonal antibodies have been raised against different GPCRs include those against β_1 and β_2 adrenergic (Moxham *et al.*, 1986), muscarinic (Luetje *et al.*, 1987), luteinizing hormone (Vuhai-Luuthi *et al.*, 1990), somatostatin (Nakabayashi & Nakabayashi, 1992) and glucagon (Iwanji & Vincent, 1990) receptors. Subsequent structural characterization of the receptor proteins involves the proteins being crystallized as complexes with the monoclonal antibodies or antigen-binding domains (Fab, Fab′ or Fv, depending on the cleavage protocol) derived from these antibodies and there are also examples where this has been successfully carried out (Ostermeier *et al.*, 1995; Sohi *et al.*, 1996; Liu *et al.*, 1996). In some of these cases, the co-crystallization method has resulted in success where standard crystallization experiments have failed (Ostermeier *et al.*, 1995; Liu *et al.*, 1996).

In this work, we report the sequencing, crystallization and X-ray crystallographic structure determination of the Fab fragment of hGR-2 F6, a monoclonal antibody raised against intact human glucagon receptor (Skovgaard, 1996). This receptor belongs to the secretin class of the GPCR superfamily, which are important receptors in the fields of molecular endocrinology and pharmacology. The secretin receptor family is distinct in having an extra domain of approximately 120 residues in length located on the extracellular N-terminus of the heptahelical transmembrane domain. This domain is known to be critical for hormone binding and recognition (Wilmen *et al.*, 1996, 1997). In addition, the first extracellular loop of the transmembrane domain also plays a role (Vilardaga *et al.*, 1996). The N-terminal domain adopts a globular protein fold that is stabilized by three disulfide bridges (Munro *et al.*, 2000). However, no crystal structure has been determined for any of these N-terminal domains and there is no significant sequence similarity to any other protein of known structure.

The natural ligand of the receptor is glucagon, a polypeptide hormone of 29 amino-acid residues in length that is generated by proteolytic cleavage of preproglucagon, a precursor of several mammalian polypeptide hormones expressed in intestinal cells and the alpha cells of the pancreas. The primary function of glucagon is to control glucose production in the liver (Girard, 1995). The liver stores glycogen, which is converted to glucose by the enzymes of the glycogenolysis cascade (Girard, 1995), which in turn is under the control of the GPCR specific for glucagon located at the hepatocyte cell surface. In view of the importance of regulating glucose levels in the body, especially in diseases like diabetes, where glucose concentration can rise to pathological levels, the glucagon receptor has been a major focus of interest for the pharmaceutical industry.

The structure of the specific anti-glucagon-receptor antibody described here is the beginning of a much larger series of experiments which will hopefully lead to the structure of the glucagon receptor itself. Once this structure has been determined, we will not only be able to understand the way in which the receptor functions, but we will also gain insights into the important mechanism of how antagonists work in general.

2. Methods

2.1. Production and characterization of monoclonal antibody

Four alternative types of antigen were investigated (Skovgaard, 1996) as a way of generating monoclonal antibodies against the human glucagon receptor: (*a*) synthetic peptides derived from the glucagon receptor, (*b*) a truncated receptor expressed in *Escherichia coli*, (*c*) antibodies to glucagon (anti-idiotypic antibody) and (*d*) intact membrane-bound receptor. Of these, only the latter method (*d*) was successful. RBF mice were immunized with a preparation of BHK cells expressing the recombinant human glucagon receptor and the spleen cells were fused with Fox-NY myeloma cells. The resultant hybridomas were screened using scintillation proximity assays (SPA) for the production of specific human glucagon-receptor antibodies; a monoclonal antibody which recognizes the native human glucagon receptor was selected. This antibody (hGR-2 F6) was shown to belong to class $IgG_{1-\kappa}$ (Skovgaard, 1996). Characterization of hGR-2 F6 was performed using an inhibition SPA. Increasing amounts of hGR-2 F6 inhibited binding of ^{125}I-glucagon to the glucagon receptor. Quantitative inhibition assays showed that hGR-2 F6 bound to the human glucagon receptor with about ten times the affinity of the endogenous ligand glucagon, while the affinity for the rat receptor was ten times lower than that of glucagon (Skovgaard, 1996). The cross reactivity against the glucagon-like peptide-1-(7,36) (GLP-1) receptor was also tested using inhibition SPA. Binding of ^{125}I-GLP1 to the GLP-1 receptor was not inhibited by adding an increasing amount of hGR-2 F6.

hGR-2 F6 was produced in protein-free medium using hollow-fibre technology and purified by protein-A affinity chromatography (Pharmacia). Binding studies of hGR-2 F6 to a series of glucagon/GLP1 receptor chimeras have demonstrated that the epitope is of a discontinuous conformational-dependent type comprising regions of the extracellular N-terminal domain and the first extracellular loop of the transmembrane domain of the glucagon receptor (Skovgaard, 1996).

2.2. Cloning and sequencing of Ig heavy and light chains

Total RNA was isolated from the above-mentioned RBF-Fox-NY hybridoma cell line using QIAshredder and RNeasy (Qiagen). Oligo-dT-primed cDNA was produced using Superscript 2 (GIBCO BRL) according to the manufacturer's instructions. PCR amplification of Ig heavy and light chains were performed using multiple primers as described by

Engberg *et al.* (1996). PCR products were cloned into the TA cloning vector pCRII (Invitrogen). 12 clones from each of the PCR reactions were selected for DNA-sequence analysis on an ABI377 DNA sequencer using the dRhodamine cycle sequencing kit (Perkin Elmer).

2.3. Sequence analysis and construction of molecular models

An open reading frame for the heavy chain was found which showed strong similarity to a range of heavy-chain sequences from kappa antibodies as shown by a *BLAST* (Altschul *et al.*, 1990) search using an in-house version of the *SRS*5 package (Etzold & Argos, 1993*a*,*b*). The most homologous of these sequences, with 87.50% sequence identity, was that of the human monoclonal anti-staphylococcal nuclease. A crystal structure for the Fab derived from this antibody (Protein Data Bank code 1nsn) has been determined to 2.9 Å resolution (Bossart-Whitaker *et al.*, 1995). The heavy chain of this Fab was used as a template for constructing a model of the heavy chain of hGR-2 F6 using the alignment shown in Fig. 1(*a*) and the *BLDPIR* homology builder in the *WHATIF* package (Vriend, 1990).

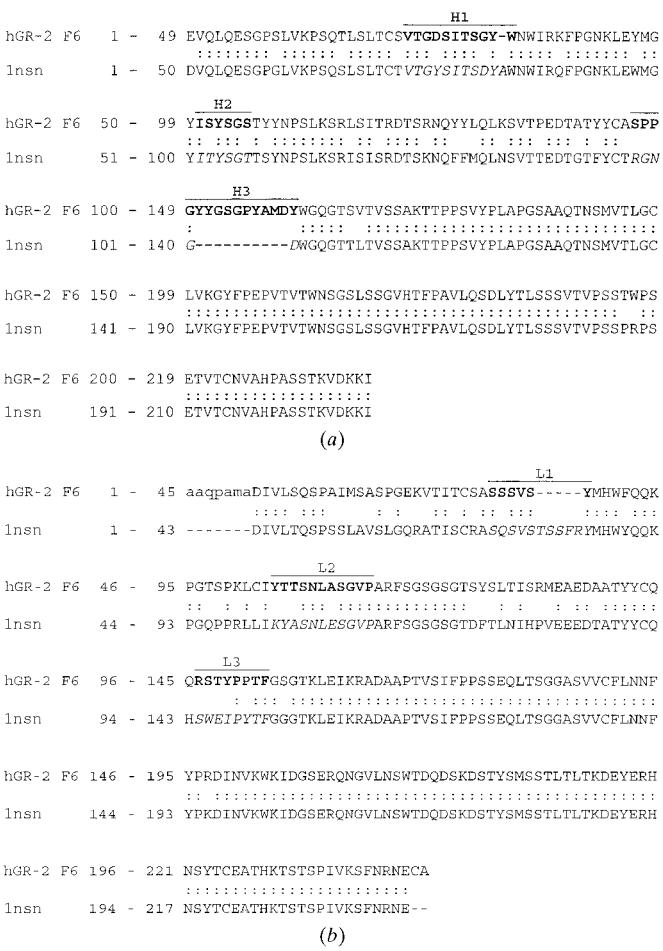

Figure 1
(*a*) Alignment of the heavy chain of hGR-2 F6 Fab with the corresponding domain of 1nsn. Residues in bold and italics correspond to the CDRs of hGR-2 F6 Fab and 1nsn, respectively. (*b*) Alignment of light chain of hGR-2 F6 Fab with the corresponding domain of 1nsn. Residues in bold and italics correspond to the CDRs of hGR-2 F6 Fab and 1nsn, respectively. Residues in lower case in hGR-2 F6 Fab are not seen in the electron density.

In the case of the light chain, two DNA sequences were found that putatively correspond to the light chain. For each of these two DNA sequences, the six protein sequences obtained by forward and backward translation with all three frameshifts (using the Wisconsin *GCG* package) were analysed for sequence similarity with the light chain of 1nsn. The identities of these six sequences were 17.95, 19.89, 17.65, 16.37, 81.60 and 16.58% for the first DNA sequence and 14.15, 13.46, 15.33, 68.31, 48.04 and 16.00% for the second DNA sequence. The strongest of these had an almost identical chain length to the light chain of 1nsn, the only difference being a pentapeptide deletion in complementarity-determining region (CDR) L1[2] (Fig. 1*b*). A model of the light chain of hGR-2 F6 was constructed on the 1nsn light-chain template in the same way as for the heavy chain.

Both models were energy minimized in an octagonal water box using the *GROMOS*87 program (Van Gunsteren & Berendsen, 1987). This model was subsequently used as an aid in chain tracing (see below).

2.4. Protein preparation and crystallization

Fab fragments were generated from the intact IgG monoclonal antibody by papain digestion (at pH 5.5) for 4 h at 310 K. Undigested IgG was removed by gel filtration (Pharmacia S75) and subsequent separation of the Fab and Fc fragments was achieved by MonoQ ion-exchange chromatography. Final purification of the Fab was performed on a MonoS column and pure Fab was eluted from the column, pooled and concentrated to 10 mg ml^{-1} in 10 m*M* Tris–HCl pH 8.0. Single crystals suitable for diffraction analysis were obtained using the sitting-drop vapour-diffusion method. Drops were composed of 0.6 µl 10 mg ml^{-1} Fab plus 0.2 µl reservoir solution [24%(*w*/*w*) polyethylene glycol 2000 monomethylether (PEG 2K MME) in 100 m*M* Tris–HCl pH 8.5]. Crystals appeared within 2–3 weeks.

2.5. X-ray data collection

The crystals were immersed in a cryo-buffer consisting of 35%(*w*/*w*) PEG 2K MME and 100 m*M* Tris pH 8.5. Data were collected from a single flash-frozen crystal at 100 K using an oscillation range of 1.2° and a crystal-to-detector distance of 307 mm. The crystals diffract to 2.1 Å resolution on station 9.5 at the SRS, Daresbury, England. The data were integrated and reduced using *DENZO* and *SCALEPACK* (Otwinowski, 1993). The crystals belong to the orthorhombic space group $P2_12_12$ and have unit-cell parameters a = 76.14, b = 133.74, c = 37.46 Å, with a single Fab molecule per crystallographic asymmetric unit. The final data set comprises 98.1% of the reflections in the resolution range 20–2.1 Å (22 946 unique

[2] L1, L2, L3, H1, H2 and H3 are the names of the individual CDRs, with L indicating that they derive from the light chain and H from the heavy chain of the Fab.

Table 1
Data-collection and processing statistics.

Values in parentheses are for the highest resolution shell (2.14–2.1 Å)

Collection site	SRS, Daresbury, station 9.5
Wavelength (Å)	0.92
Temperature (K)	100
Space group	$P2_12_12$
Unit-cell parameters (Å)	
a	76.14
b	133.74
c	37.46
No. of reflections measured	173940
No. of unique reflections	22946
Overall R_{merge}† (%)	5.3 (31.9)
Completeness	98.1 (95.4)
Multiplicity	4
Resolution limits	20.0–2.1Å
$I/\sigma(I)$	10.4 (2.6)

† $R_{merge} = \sum|I - \langle I\rangle|/\sum\langle I\rangle$.

reflections) and has a merging *R* factor of 5.3%. A summary of the data-collection parameters is given in Table 1.

2.6. Crystal structure determination

The structure of the Fab was determined by the molecular-replacement method using *AMoRe* (Navaza, 1994). The coordinates of the variable light and heavy chain of the Fab 1nsn (all atoms included) were used as a search model. The rotation and translation functions, using data in the resolution range 8–4 Å, gave a single clear solution (2σ above the next highest peak), which is consistent with a single Fab molecule in the asymmetric unit. Following rigid-body refinement with *AMoRe* (15–3.5 Å), the final solution had a correlation coefficient of 44.7 and an *R*-factor value of 52.6%.

2.7. Chain tracing and refinement

Chain tracing was carried out using the modelling program *QUANTA* (Molecular Simulations Inc.). The model obtained from molecular modelling was found to be useful as an aid in fitting the correct sequence to the electron density. After including the two deletions and one insertion (see Figs. 1*a* and 1*b*) and replacing the various residues that differed between the two structures, the Fab monomer was refined using restrained refinement with *REFMAC* (Murshudov *et al.*, 1997). This reduced the conventional *R* factor from 42.3 to 28.9% (R_{free} = 36.6%). Solvent molecules were automatically placed and refined using *REFMAC* cycled with *ARPP* (Lamzin & Wilson, 1993) and minor side-chain adjustments were made following periodic manual inspections of the model in *QUANTA*. At each stage of the refinement, 20 cycles of *REFMAC* were carried out and the progress of the refinement was assessed using R_{free}.

2.8. Superposition studies

The hypervariable regions of the final model were compared with other known antibody structures in order to classify the CDRs according to the standard canonical forms as defined by Chothia *et al.* (1989). The CDRs were superposed onto those from HyHEL-10 and HyHEL-5 (Padlan *et al.*, 1989) using *LSQKAB* (Kabsch, 1976).

3. Results

3.1. Sequencing

The sequences for the heavy and light chains for hGR-2 F6, as determined experimentally (see §2) and their alignments with the 1nsn sequences are shown in Figs. 1(*a*) and 1(*b*). The CDR residues for hGR-2 Fab are in bold. The percentage sequence identities between hGR-2 F6 and 1nsn are 82% for the light chain and 86% for the heavy chain.

3.2. Overall three-dimensional structure

The hGR-2 F6 Fab exhibits the typical immunoglobulin fold (Fig. 2). Most of the model is well defined by the electron density. However, for 12 residues (H103–H106, H138–H141 and L200–L202) which form two loop regions of the heavy chain and a loop of the light chain, the electron density is only partially ordered and is almost uninterpretable. These observations are consistent with the structures of several other previously reported Fab molecules (*e.g.* Fischmann *et al.*, 1991; Mizutani *et al.*, 1995). An example of the electron-density map at CDR L1 is shown in Fig. 3.

The final model for the hGR-2 F6 Fab consists of 3319 protein atoms and 380 water molecules, with an *R* value of 21.7% for all data in the resolution range 20.0–2.10 Å. The R_{free} value is relatively high (31.5%) for a 2.1 Å structure and this probably reflects the partially ordered nature of the three loops mentioned above. The model was checked for stereochemical

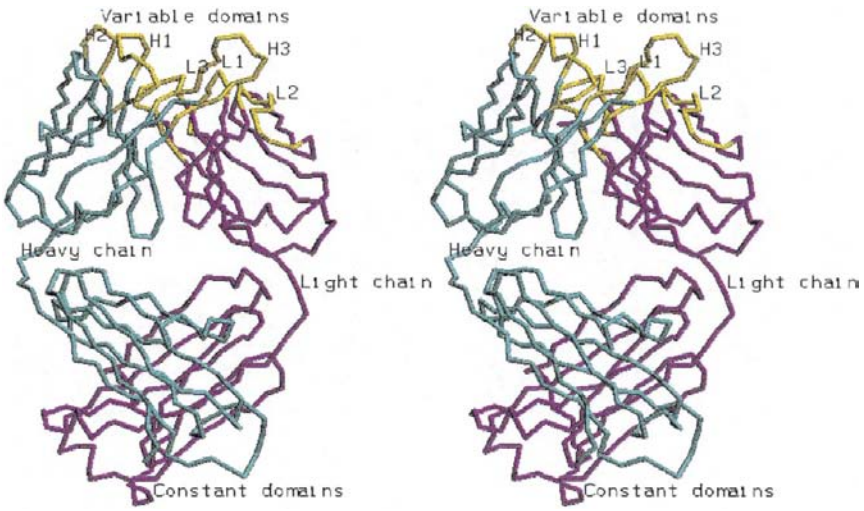

Figure 2
Stereo diagram of the C^{α} trace of the Fab monomer.

correctness using the program *PROCHECK* (Laskowski *et al.*, 1993). Ramachandran plots (Ramachandran *et al.*, 1963) for both the heavy and light chains show that most residues lie in or near the allowed conformational regions (98.1% of residues are in allowed regions). There are several residues that fall outside the allowed region of φ/ψ torsional angle space as defined in *PROCHECK* (Laskowski *et al.*, 1993). These include Thr50, Asn156, Ser202 and Cys213 in the light chain and Lys64, Tyr102 and Asn142 of the heavy chain. All these residues, apart from Thr52 (L), lie in poorly ordered regions of the structure. In contrast, Thr52 is located in the L2 CDR, which is well defined in the electron-density maps. The unusual main-chain conformation of this residue is probably a consequence of its location in a classic γ turn at the apex of the L2 hypervariable loop.

The mean coordinate error was estimated by *SFCHECK* (Vaguine *et al.*, 1999) to be 0.241. The highest *B* factors are in the solvent-exposed loop areas of the heavy chain, which indicate their flexibility and disorder. There is a typical kink (Spada *et al.*, 1998) at the proline residue in the sequence QSPAI in the first strand of the V_L domain. The elbow angle for hGR-2F6 Fab is 111.3°, which is slightly larger than the elbow angle of 107.7° for 1nsn. This difference in the elbow angles might explain the relatively low correlation coefficient obtained in *AMoRe* when using the intact 1nsn as a search model. Refinement and model-validation statistics of the final hGR-2F6 Fab model are presented in Table 2.

3.3. The antigen-binding site

The conformations of the CDR loops were analysed according to the scheme of Chothia *et al.* (1989). The five CDRs, L1, L2, L3, H1 and H2, superimpose well onto standard canonical CDR loops. All were most similar to the CDRs of HyHEL-10 (Padlan *et al.*, 1989) apart from L1, which compares better with the corresponding CDR from HyHEL-5 (see Table 3).

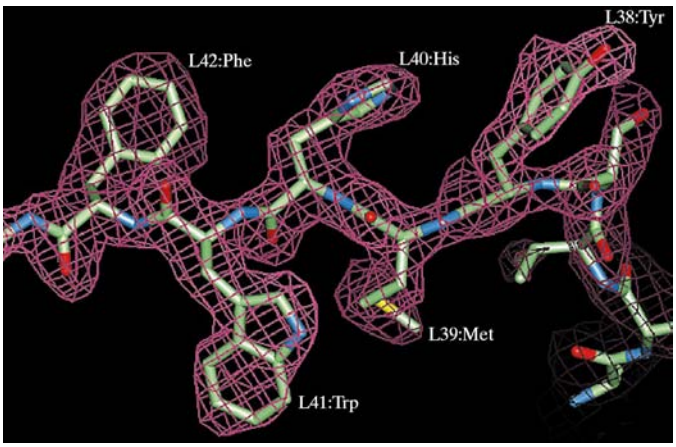

Figure 3
Final α_A-weighted ($2mF_o - DF_c$) electron-density map overlaid on the final model. The region shown is in the vicinity of CDR H1 and the map is contoured at 1σ.

The H3 loop resembles a β-hairpin but is somewhat distorted owing to two consecutive proline (both *trans*) residues at the N-terminus of the turn. The H3 loop cannot be analysed according to the scheme above since generally in antibodies H3 loops are the most polymorphic of the CDRs in terms of length and sequence diversity and are very dissimilar between different antibody structures. However, 'H3 rules', which were introduced recently by Shirai *et al.* (1999) can be

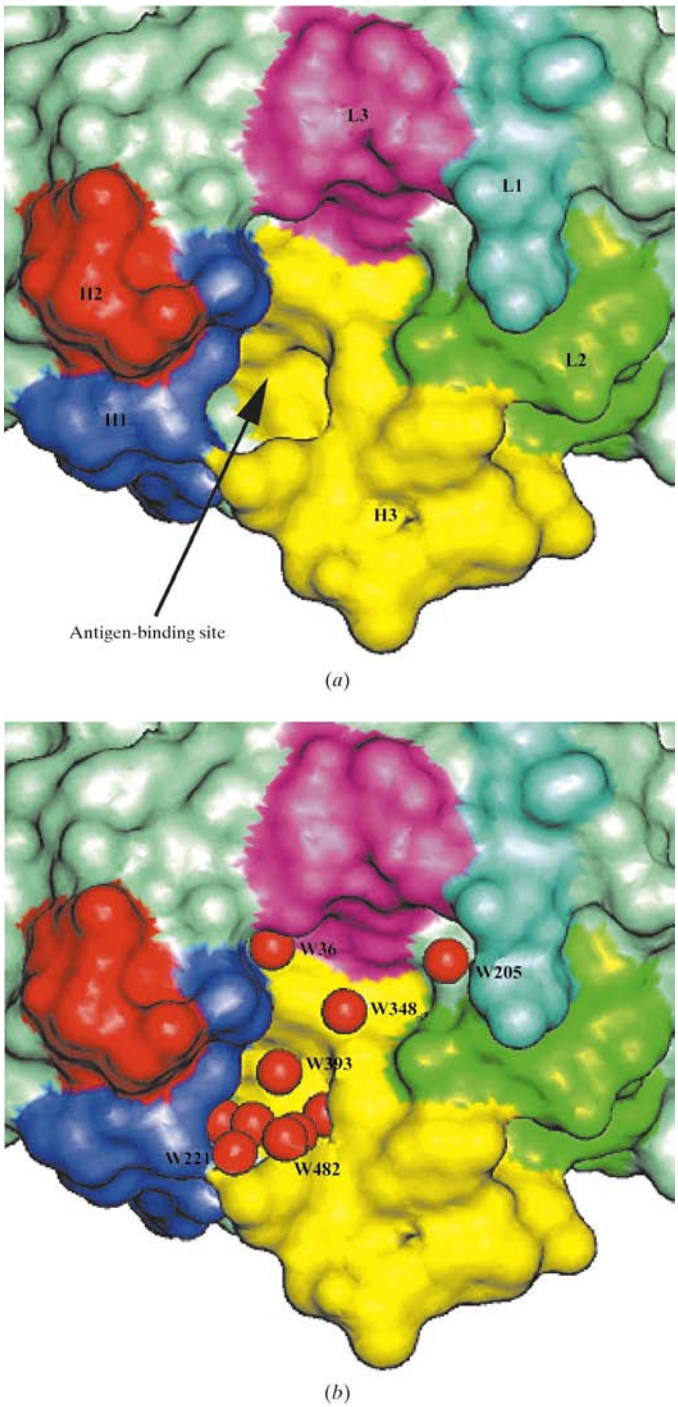

Figure 4
Surface representation of the antigen-combining site viewed in (*a*) the absence and (*b*) the presence of bound solvent molecules. The surface was calculated using *QUANTA* (Molecular Simulations Inc.).

Table 2
Refinement statistics.

Resolution range (Å)	20.0–2.1
No. of reflections used	22425
Crystallographic R factor† for all‡ data (%)	21.7
R_{free}§ for all data (%)	31.5
No. of Fab atoms	3319
No. of solvent molecules	380
Average B value for V_L and C_L atoms (Å^2)	40.6
Average B value for V_H and C_H atoms (Å^2)	45.5
Average B value for the solvent molecules (Å^2)	49.4
R.m.s. deviations from ideality	
Bond lengths (Å)	0.011
Bond angles (°)	2.9

† Crystallographic R factor = $\sum||k|F_{obs}| - |F_{calc}||/\sum k|F_{obs}|$, where F_{obs} and F_{calc} are the observed and calculated structure-factor amplitudes, respectively. ‡ No σ-cutoff was applied to the data. § R_{free} is the crystallographic R factor calculated for a subset of randomly selected reflections (5%) not used in the phasing process (Brünger, 1992).

used to classify H3 and the results of this classification are shown in Table 4. The residues L46 and L49 are class descriptors related to the types of residue in the light-chain loops which abut the H3 loop. In the class in which L49 is a Lys residue, a salt bridge is formed with the Asp residue in the $(n-1)$th position in the H3 loop. These key residues are Leu and Tyr, respectively, in hGR-2 F6 and are Leu and Lys, respectively, in 1nsn, which places each of these two H3 loops into a different class: K (kinked) in the case of the latter and E (extended) in the case of hGR-2 F6.

A total of 56 residues are associated with the CDRs and together they represent a solvent-accessible area of 1460 Å^2, which accounts for only 6.2% of the total accessible area for the complete Fab molecule. As a result, the antigen-binding surface forms a shallow cleft of approximate dimensions 14 Å long, 11 Å wide and 6 Å deep which lies perpendicular to the heavy- and light-chain interface. This is typical of most antigen-binding sites and similar-sized clefts have been observed in the crystal structures of several protein–antigen complexes (Benjamin, 1991; Laskowski *et al.*, 1996). The dimensions of the cleft suggest that only relatively small molecules/peptides will fit into the antigen-binding site and much larger peptides will protrude out of the site. There are also two deeper grooves located in the antigen-binding site: one is beside CDR H1 and the other is located near CDR L3 (see Fig. 4*a*). In this unliganded structure, five water molecules are buried within these grooves which help to hold the CDRs in the canonical forms they adopt *via* hydrogen bonds and van der Waals interactions (see Fig. 4*b*). In total, there are ten solvent molecules located in the antigen-binding site, which presumably occupy the space where an antigen would bind or even participate in the binding interaction. Eight of these water molecules interact directly with residues of the CDRs; the other two waters interact indirectly *via* hydrogen bonds with other solvent molecules.

4. Discussion

This work describes the structure of an antibody to the human glucagon receptor which has been shown to be highly specific for this receptor and to act as a competitive antagonist (Skovgaard, 1996). The overall fold is typical of an immunoglobulin fold. Of the CDRs, all six have been fully defined, although CDR H3 is only partially ordered. Between hGR-2 F6 Fab and the template 1nsn, which was used in modelling, CDR H3 shows the largest differences in conformation, having a large insertion of ten residues relative to the latter. Therefore, the model could not be of any assistance in chain tracing in this region. Nevertheless, its geometry could be ascertained from the electron density to be in the form of a somewhat distorted β-hairpin.

Table 3
Results of superposition of CDRs with backbone atoms (N, C$^\alpha$, C, O), calculated using *LSQKAB*.

Loop	Compared with	Canonical form	R.m.s.d. (Å)
L1	L1-HyHEL-5	1	0.91
L2	L2-HyHEL-10	1	1.10
L3	L3-HyHEL-10	1	0.89
H1	H1-HyHEL-10	1′	1.02
H2	H2-HyHEL-10	1	0.95

Five of the CDRs (L1, L2, L3, H1 and H2) conform to the standard canonical forms as described by Chothia *et al.* (1989). The H3 loop could be classified in terms of sequence and length according to the 'H3 rules' of Shirai *et al.* (1999). This CDR may change its geometry upon binding to antigen, since it is a large loop in a structure where there is no bound ligand to restrain its movement. Conformational changes that take place on binding in ligand-recognition loops or surfaces are a very widely observed phenomenon, for example, in antibodies (Rini *et al.*, 1992), enzymes (Krekel *et al.*, 1999) and nuclear receptors (Holmbeck *et al.*, 1998); thus, we anticipate that the H3 loop may well change its conformation in the complex with the epitope.

Certain amino acids have a higher probability of being located in the antigen-binding site (Mian *et al.*, 1991). Tyr, Ser and Trp are the most frequently found, whereas Gln, Val and Leu are more uncommon. In the CDRs of hGR-2 F6 Fab, collectively, there are seven tyrosines, ten serines and one tryptophan. It is thought that the positions of the hydroxyl groups of these seven tyrosine residues and ten serine residues are very important for the binding of the antigen to the antibody. The side chain of the single tryptophan, located on CDR-H1, could be involved in forming aromatic stacking interactions with hydrophobic/aromatic residues of the antigen upon binding. Likewise, the tyrosines can also participate in these types of interactions or in hydrogen bonding. Charged residues are often involved in specific interactions with the antigen. There are two potentially charged residues on CDR L3 (GlnL89 and ArgL90), one on CDR H1 (AspH27) and one (ArgH71) on CDR H2 which are in the central region of the combining site. These might be involved in specific charged interactions with acidic residues on the human glucagon-receptor protein.

In recent work, synthetic compounds have been studied as potential effectors of secretin receptors. Novel triarylimidazole and triarylpyrrole glucagon-receptor antagonists

Table 4
Classification of CDR-H3.

In this table, +/− indicates whether the Fab structure is a complex with antigen (+) or free (−), the first three letters of the sequence represent the amino-acid residues preceding the H3 loop, followed by the H3 sequence in given in parentheses; W is the fully conserved residue immediately following the H3 loop. L and K/Y are the identities of the light-chain residues L46 and L49, respectively. *n* corresponds to the total length of the H3 loop and the assignment of the H3 loop to the kinked (K) or extended (E) class is given (Shirai *et al.*, 1999).

Antibody name	PDB code	+/−	Sequence	L46	L49	*n*	Class
N10	1nsn	+	CTR (GNGD) W	L	K	4	K
HGR-2 F6	1dqd	−	CAS (PPGYYGSGPYAMDY) W	L	Y	14	E

have been described (Cascieri *et al.*, 1999). These do not displace the endogenous ligand, as it binds deep in a binding pocket in the receptor. In contrast, it has been shown that for various members of the secretin-family receptors, including by analogy/homology the glucagon receptor, the hormone binds mainly to the extracellular N-terminal domain (Wilmen *et al.*, 1996) and to the extracellular loops (Vilardaga *et al.*, 1996). While the hormone may penetrate somewhat into the interior of the receptor, it clearly does not overlap the reported binding site for synthetic ligands.

It is known that HGR-2 Fab is a competitive antagonist of the receptor and as such displaces the hormone. Although it has not been shown whether the antibody also displaces the synthetic ligands, it would seem reasonable at this stage to eliminate the possibility that the CDRs of the antibody penetrate deep into the interior of the receptor. It is more likely that it competes with the sites on the extracellular regions of the receptor referred to earlier. However, we do not at this stage know the exact identity of the epitope. A range of potential epitopes have been designed and synthesized and are currently being screened for binding to the antibody. Once available, we will use the structural information from the complex of the antibody and a receptor epitope as a guide to the design of new highly specific antagonists. Future work will focus on using X-ray crystallography to study new complexes between the receptor epitope(s) and the Fab in order to determine the conformation of a peptide which has antagonist action.

Mutants of glucagon itself have been studied in order to identify possible sites of interaction between the hormone and the receptor (Rodbell *et al.*, 1971; Frandsen *et al.*, 1981; Gysin *et al.*, 1986; Krztansky *et al.*, 1986; Andreu & Merrifield, 1987; Zechel *et al.*, 1991; Dharanipragada *et al.*, 1993; Unson *et al.*, 1996; Montrose-Rafizadeh *et al.*, 1997; Sturm *et al.*, 1997; Parker *et al.*, 1998). These studies have not been particularly useful in terms of new ligand design, but they have facilitated the mapping of sites on the receptor that are important for ligand binding. These results support a model in which the hormone interacts at several regions on the N-terminal globular domain and on the first extracellular loop of the transmembrane domain.

Finally, the ultimate goal would be a crystal structure of the entire receptor–Fab complex. This will involve co-crystallizing the hGR-2 F6 Fab domain with the human glucagon-receptor protein. Until then, one can only speculate how the H3 loop and the other CDRs bind to the receptor using models of the receptor and a knowledge of the residue types in the loops as described above. We hope that the structural details of the interaction between the CDRs of the antibody and the receptor may be of value in designing low molecular-weight compounds that block this receptor.

References

Altschul, S. F., Gish, W., Miller, W., Myers, E. W. & Lipman, D. J. (1990). *J. Mol. Biol.* **215**, 403–410.
Andreu, D. & Merrifield, R. B. (1987). *Eur. J. Biochem.* **164**, 585–590.
Benjamin, D. C. (1991). *Int. Rev. Immunol.* **7**, 149–164.
Bossart-Whitaker, P., Chang, C. Y., Novotny, J., Benjamin, D. C. & Sheriff, S. (1995). *J. Mol. Biol.* **253**, 559–575.
Brünger, A. T. (1992). *Nature (London)*, **355**, 472–475.
Cascieri, M. A., Koch, G. E., Ber, E., Sadowski, S. J., Louizides, D., de Laszlo, S. E., Hacker, C., Hagmann, W. K., MacCoss, M., Chicchi, G. G. & Vicario, P. P. (1999). *J. Biol. Chem.* **274**, 8694–8697.
Chothia, C., Lesk, A. M., Tramontano, A., Levitt, M., Smith-Gill, S. J., Air, G., Sheriff, S., Padlan, E. A., Davies, D., Tulip, W. R., Colman, P. M., Spinelli, S., Alzari, P. M. & Poljak, R. J. (1989). *Nature (London)*, **342**, 877–883.
Dharanipragada, R., Trivedi, D., Bannister, A., Siegel, M., Tourwe, D., Mollova, N., Schram, K. & Hruby, V. J. (1993). *Int. J. Pept. Protein Res.* **42**, 68–77.
Engberg, J., Andersen, P. S., Nielsen, L. K., Dziegiel, M., Johansen, L. K. & Albrechtsen, B. (1996). *Mol. Biotechnol.* **6**, 287–310.
Etzold, T. & Argos, P. (1993*a*). *Comput. Appl. Biosci.* **9**, 49–57.
Etzold, T. & Argos, P. (1993*b*). *Comput. Appl. Biosci.* **9**, 59–64.
Fischmann, T. O., Bentley, G. A., Bhat, T. N., Boulot, G., Mariuzza, R. A., Phillips, S. E. V., Tello, D. & Poljak, R. J. (1991). *J. Biol. Chem.* **266**(20), 12915–12920.
Frandsen, E. K., Grønvald, F. C., Heding, L. G., Johansen, N. L., Lundt, B. F., Moody, A. J., Markussen, J. & Volund, A. (1981). *Hoppe-Seyler's Z. Physiol. Chem.* **362**, 665–677.
Girard, J. (1995). *Diabetes*, **35**, 1–19.
Gysin, B., Johnson, D. G., Trivedi, D. & Hruby, V. J. (1986). *J. Med. Chem.* **30**, 1409–1415.
Holmbeck, S. M., Foster, M. P., Casimiro, D. R., Sem, D. S., Dyson, H. J. & Wright, P. E. (1998). *J. Mol. Biol.* **281**, 271–284.
Iwanji, W. & Vincent, A. C. (1990). *J. Biol. Chem.* **265**, 21302–21308.
Kabsch, W. (1976). *Acta Cryst.* A**32**, 922–923.
Krekel, F., Oecking, C., Amrhein, N. & Macheroux, P. (1999). *Biochemistry*, **38**, 8864–8878.
Krztansky, J. L., Trivedi, D. & Hruby, V. J. (1986). *Biochemistry*, **25**, 3833–3839.
Lamzin, V. S. & Wilson, K. S. (1993). *Acta Cryst.* D**49**, 129–147.
Laskowski, R. A., Luscombe, N. M., Swindells, M. B. & Thornton, J. M. (1996). *Protein Sci.* **5,** 2438–2452.
Laskowski, R. A., MacArthur, M. W., Moss, D. S. & Thornton, J. M. (1993). *J. Appl. Cryst.* **26**, 283–291.
Liu, J., Tse, A. G., Chang, H. C., Liu, J. H., Wang, J., Hussey, R. E., Chishti, Y., Rheinhold, B., Spoerl, R., Nathenson, S. G., Sacchettini, J. C. & Reinherz, E. L. (1996). *J. Biol. Chem.* **271**, 33639–33646.
Luetje, C. W., Brunwell, C., Norman, M. C., Peterson, G. L., Schimerlik, M. I. & Nathanson, N. M. (1987). *Biochemistry*, **26**, 6892–6896.
Mian, I. S., Bradwell, A. R. & Olson, A. J. (1991). *J. Mol. Biol.* **217**, 133–151.

Mizutani, R., Miura, K., Makayama, T., Shimada, I., Arata, Y. & Satow, Y. (1995). *J. Mol. Biol.* **254**(2), 208–222.
Montrose-Rafizadeh, C., Yang, H., Rodgers, B. D., Beday, A., Pritchette, L. A. & Eng, J. (1997). *J. Biol. Chem.* **272**, 21201–21206.
Moxham, C. P., George, S. H., Graziano, M. P., Brandwein, H. J. & Malbon, C. C. (1986). *J. Biol. Chem.* **268**, 14562–14570.
Munro, R. E. J., Taylor, W. R. & Bywater, R. P. (2000). Submitted.
Murshudov, G. N., Vagin, A. A. & Dodson, E. J. (1997). *Acta Cryst.* D**53**, 240–255.
Nakabayashi, I. O. & Nakabayashi, H. (1992). *Hybridoma*, **11**, 789–794.
Navaza, J. (1994). *Acta Cryst.* A**50**, 157–163.
Ostermeier, C., Iwata, S., Ludwig, B. & Michel, H. (1995). *Nature Struct. Biol.* **2**, 842–846.
Otwinowski, Z. (1993). *Proceedings of the CCP4 Study Weekend. Data Collection and Processing*, edited by L. Sawyer, N. Isaacs & S. Bailey, pp. 56–62. Warrington: Daresbury Laboratory.
Padlan, E. A., Silverton, E. W., Sherriff, S., Cohen, G. H., Smith-Gill, S. J. & Davies, D. R. (1989). *Proc. Natl Acad. Sci. USA*, **86**, 5938–5942.
Parker, J. C., Andrews, K. M., Rescek, D. M., Massefski, W. Jr, Andrews, G. C., Contillo, L. G., Stevenson, R. W., Singleton, D. H. & Suleske, R. T. (1998). *J. Pept. Res.* **52**, 398–409.
Ramachandran, G. N., Ramakrishnan, C. & Sasisekharan, V. J. (1963). *J. Mol. Biol.* **7**, 95–99.
Rini, J. M., Schulze-Gahmen, U. & Wilson, I. A. (1992). *Science*, **255**, 959–965.
Rodbell, M., Birnbauemer, L. Pohl, S. L. & Sundby, F. (1971). *Proc. Natl Acad. Sci. USA*, **68**, 909–913.
Shirai, H., Kidera, A. & Nakamura, H. (1999). *FEBS Lett.* **455**, 188–197.
Skovgaard, R. N. (1996). Thesis: *Monoclonal Antibody to Human Glucagon Receptor. A Glucagon-Receptor Antagonist.* Novo Nordisk A/S, Bagsværd, Denmark & August Krogh Institute, University of Copenhagen, Denmark.
Sohi, M. K., Corper, A. L., Wan, T., Steinitz, M., Jefferis, R., Beale, D., He, M., Feinstein, A., Sutton, B. J. & Taussig, M. J. (1996). *Immunology*, **88**, 636–641.
Spada, S., Honegger, A. & Pluckthun, A. (1998). *J. Mol. Biol.* **283**, 395–407.
Sturm, N. S., Hutzler, A. M., David, C. S., Azizeh, B. Y., Trivedi, D. & Hruby, V. J. (1997). *J. Pept. Res.* **49**, 293–299.
Unson, C. G., Cypess, A. M., Wu, C. R., Goldsmith, P. K., Merrifield, R. B. & Sakmar, T. P. (1996). *Proc. Natl Acad. Sci. USA*, **93**, 310–315.
Vaguine, A. A., Richelle, J. & Wodak, S. J. (1999). *Acta Cryst.* D**55**, 191–205.
Van Gunsteren, W. F. & Berendsen, H. J. C. (1987). *GROMOS: Groningen Molecular Simulation Computer Program Package.* University of Groningen, The Netherlands.
Vilardaga, J. P., Di Paolo, F., De Neef, P., Waelbroeck, M., Bollen, A. & Robberecht, P. (1996). *Biochem. Biophys. Res. Commun.* **218**, 842–846.
Vriend, G. (1990). *J. Mol. Graph.* **8**, 52–56.
Vuhai-Luuthi, M. T., Jolivet, A., Jallal, B., Salesse, R., Bidart, J., Houllier, A., Gueochen-Mantel, A., Garnier, J. & Milgrom, E. (1990). *Endocrinology*, **127**, 2090–2098.
Wilmen, A., Göke, B. & Göke, R. (1996). *FEBS Lett.* **398**, 43–47.
Wilmen, A., Van Eyll, B., Göke, B. & Göke, R. (1997). *Peptides*, **18**, 301–305.
Zechel, C., Trivedi, D. & Hruby, V. J. (1991). *Int. J. Pept. Protein. Res.* **38**, 131–138.